Comparative Medicine
Copyright 2013
by the American Association for Laboratory Animal Science

Vol 63, No 5
October 2013
Pages 398–408

Original Research

Development of a Murine Model of Blunt Hepatic Trauma

Jean A Nemzek-Hamlin,[1,*] Haejin Hwang,[1] Joseph A Hampel,[1] Bi Yu,[2] and Krishnan Raghavendran[2]

Despite the prevalence of blunt hepatic trauma in humans, there are few rodent models of blunt trauma that can be used to study the associated inflammatory responses. We present a mouse model of blunt hepatic trauma that was created by using a cortical contusion device. Male mice were anesthetized with ketamine–xylazine–buprenorphine and placed in left lateral recumbency. A position of 2 mm ventral to the posterior axillary line and 5 mm caudal to the costal margin on the right side was targeted for impact. An impact velocity of 6 m/s and a piston depth of 12 mm produced a consistent pattern of hepatic injury with low mortality. All mice that recovered from anesthesia survived without complication for the length of the study. Mice were euthanized at various time points (n = 5 per group) until 7 d after injury for gross examination and collection of blood and peritoneal lavage fluids. Some mice were reanesthetized for serial monitoring of hepatic lesions via MRI. At 2 h after trauma, mice consistently displayed laceration, hematoma, and discoloration of the right lateral and caudate liver lobes, with intraabdominal hemorrhage but no other gross injuries. Blood and peritoneal lavage fluid were collected from all mice for cytokine analysis. At 2 h after trauma, there were significant increases in plasma IL10 as well as peritoneal lavage fluid IL6 and CXCL1/KC; however, these levels decreased within 24 h. At 7 d after trauma, the mice had regained body weight, and the hepatic lesions, which initially had increased in size during the first 48 h, had returned to their original size. In summary, this technique produced a reliable, low mortality, murine model that recreates features of blunt abdominal liver injury in human subjects with similar acute inflammatory response.

Abbreviation: CXCL1/KC, keratinocyte-derived chemokine.

Trauma is the most frequent cause of mortality worldwide,[11] and in cases of blunt abdominal trauma, the liver is the most frequently injured organ.[4] In humans, traumatic injuries to the liver are graded (I through VI) according to the American Association for the Surgery of Trauma Liver Injury Scale, which is based on the severity of lesions, including hematomas, lacerations and vascular disruption.[10] Parenchymal injuries (grades I through III) are more common than are major vascular injuries (grades V and VI), correlating with the greater hemodynamic stability and lower early mortality rates of parenchymal damage.[4] Although early mortality rates may be low in low-grade injuries, the overall mortality rates for abdominal traumas involving liver are greater than that of abdominal trauma without liver damage. Late mortality after liver injury is associated with immunologic dysfunction, leading to systemic inflammatory response syndrome, sepsis, and multiple-organ failure.[6]

To study the complex immune responses surrounding blunt hepatic trauma, an appropriate animal model is imperative, but few animal models of liver trauma have been described. Swine traditionally have been the preferred model because of similarity of the liver anatomy and lesions to those of human cases.[2] Nonpenetrating models have been developed in swine and involve impact by crossbow or other blunted projectiles.[20] The first rodent model of trauma was developed by positioning anesthetized rats under a column containing a flat weight.[3] In that model, the severity of injury could be adjusted by the height of the column. This model was distinctive in its use of the least sentient species to date. The large animal models and even the rat model would readily support studies of treatment modalities and the measurement of hemodynamic parameters. For extensively characterizing the immunopathology associated with liver trauma, a murine model could offer distinct advantages, including the ready availability of transgenic mice and the extensive array of reagents for immunologic studies.

The purpose of the current study was to develop a reliable and reproducible, closed abdominal, murine model of blunt hepatic trauma that is suitable for studies of posttraumatic immune dysfunction and related complications. Our first aim was to develop a low-mortality model that demonstrated gross and microscopic hepatic lesions similar to those seen in humans. The second study aim was to define selected systemic and local immune responses, including immune cell counts and cytokine levels. In addition, we examined the potential use of a noninvasive imaging technique (MRI) for the sequential evaluation of hepatic lesions.

Materials and Methods

Study design. In an initial pilot study, anesthetized mice (n = 5 per group) underwent a contusion procedure at various levels of impact and were euthanized 2 h afterward. The presence and

Received: 20 Feb 2013. Revision requested: 25 Mar 2013. Accepted: 15 Apr 2013.
[1]Unit for Laboratory Animal Medicine and [2]Department of Surgery, University of Michigan, Ann Arbor, Michigan.
[*]Corresponding author. Email: jnemzek@umich.edu

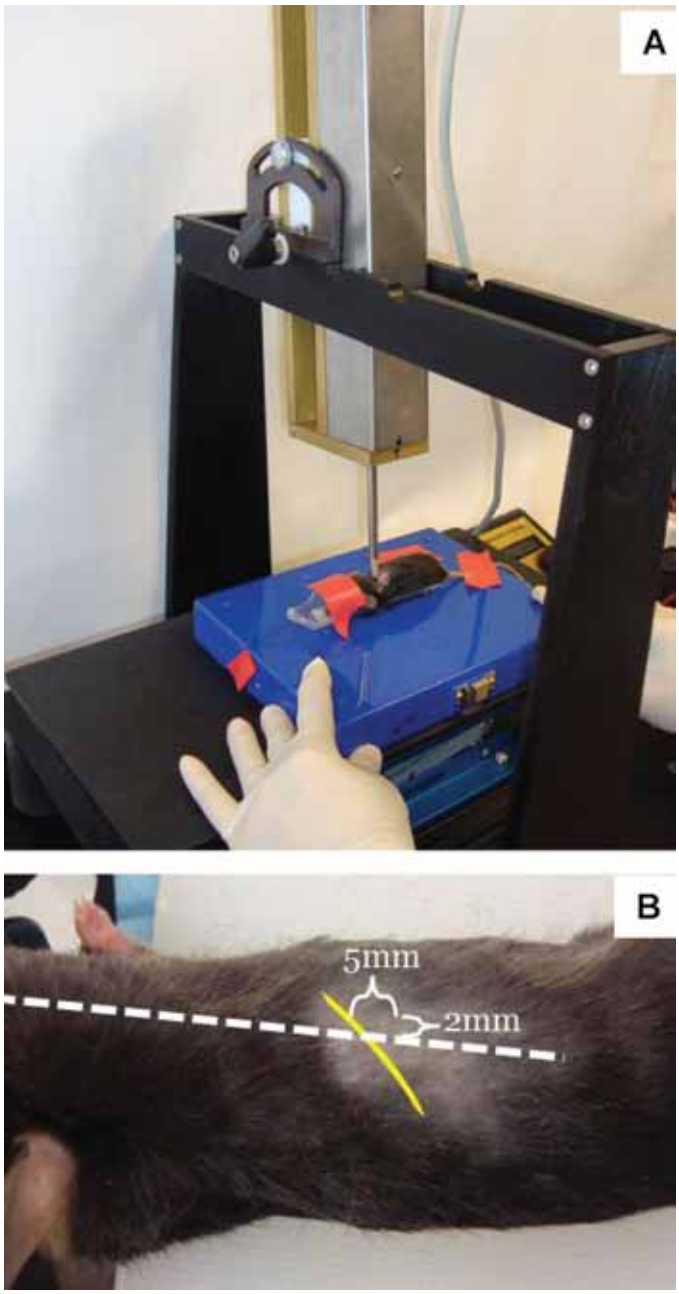

Figure 1. Techniques for delivery of impact to create liver trauma. (A) The cortical contusion device, with piston lowered to within 12 mm of the body surface of the mouse. The mouse was secured, with the right forelimb extended forward, in a modified syringe case to allow exact positioning in left lateral recumbency. (B) The correct landmarks for impact were designated by a line extended from the caudal edge of the limb and axillary skin fold (dotted white line) and a second line denoted by palpation of the costochondral arch. A point 2 mm ventral to the posterior axillary line and 5 mm caudal to the ribs was the point of impact on the right side.

pattern of injury were used to determine the impact level that yielded consistent, low-mortality injuries similar to conservatively treated hepatic injuries in human patients. Once the level of injury was established, the blunt trauma procedure was repeated on mice (n = 5 per group) that were euthanized at 2 h, 24 h, 48 h,

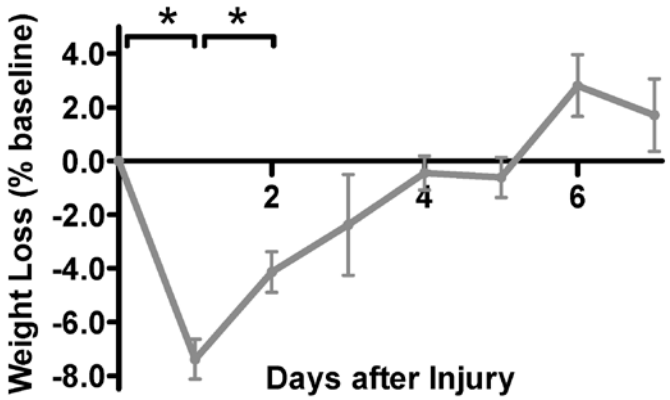

Figure 2. Weight changes for mice after blunt hepatic trauma. After induction of anesthesia, mice were positioned for precise delivery of a blunt abdominal force from a specialized cortical contusion device. There was significant (*, $P < 0.05$) loss of body weight, although less than 10%, over the first 24 h which then demonstrated a significant rebound. Data are expressed as mean ± SEM (n = 5 per group).

and 7 d after trauma to evaluate local and systemic responses to injury. A control group (n = 3) underwent identical handling, anesthesia, and analgesic administration without the contusion procedure and was euthanized at the 2-h time point.

Animals. Male C57BL/6 mice (age, 9 to 10 wk; The Jackson Laboratory, Bar Harbor, ME) were housed 5 per cage in static microisolation caging in an SPF barrier facility. Male mice were housed only with the same cagemates, and no evidence of fighting was noted. After the induction of injury, mice that were fully recovered from anesthesia were group-housed. Mice were SPF for viruses including mouse hepatitis virus, minute virus of mice, mouse parvovirus, epizootic diarrhea of infant mice virus, ectromelia virus, Sendai virus, pneumonia virus of mice, Theiler murine encephalomyelitis virus (strain GD VII), reovirus, lymphocytic choriomeningitis virus, mouse adenovirus, and polyomavirus. Mice had ad libitum access to food (Laboratory Rodent Diet 5001, PMI LabDiets, St Louis, MO) and water. After injury, mice were supplemented with Diet Gel Recovery (ClearH_2O, Portland, ME). The animal housing room was maintained on a 12:12-h light:dark cycle with constant temperature (72 ± 2 °F [22.2 ± 1.2 °C]). Mice were acclimated for at least 5 d prior to experimental use. The institution is AAALAC-accredited, and all procedures were approved by the University of Michigan's Animal Care and Use Committee.

Contusion procedure. Mice were anesthetized with ketamine (87 mg/kg; Fort Dodge Laboratories, Fort Dodge, IA) and xylazine (13 mg/kg; Akorn, Decatur, IL). Buprenorphine (0.1 mg/kg; Bedford Labs, Bedford, OH) was administered at this time and again postoperatively at 8-h intervals as needed. Once the depth of anesthesia was confirmed, mice were placed in left lateral recumbency and were shaved to permit accurate identification of landmarks. Each mouse was cradled in a modified syringe case to allow secure positioning, with the right forelimb extended forward and secured to the syringe case. Mice then were placed on the platform of the electric cortical contusion device (Custom Design and Fabrication, VCU, Richmond, VA; Figure 1 A). The anatomic placement of the impact point was 5 mm caudal to the costal margin and 2 mm ventral to a line analogous to the posterior axillary line (Figure 1 B). In humans, the posterior axillary

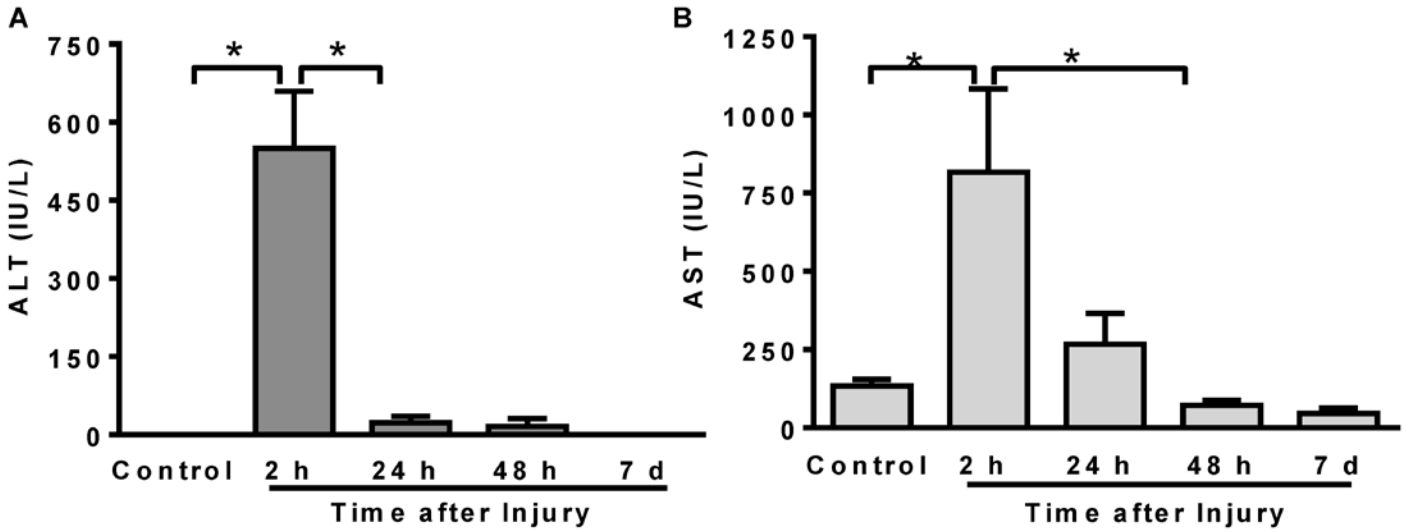

Figure 3. Plasma AST and ALT levels after blunt hepatic trauma. Mice were anesthetized for delivery of a blunt abdominal force to the right side. Within 2 h of injury, (A) ALT and (B) AST levels in plasma both were significantly (*, $P < 0.05$) elevated as compared with those in noninjured control animals. ALT levels decreased to those comparable to those of the control animals within 24 h, whereas AST levels required 48 to be significantly ($P < 0.05$) reduced. Data are expressed as mean ± SEM ($n = 5$ per group).

line extends along the side of the body from the caudal skin fold of the armpit.[21] In mice, a line extending from the caudal aspect of the extended right forelimb was designated. The device delivered a single blow to the targeted point. The piston velocity was 6 m/s, with a depth of 12 mm between the starting position of the piston and the body surface. Immediately after blunt trauma, mice were placed on a warming pad and monitored closely until recovery from anesthesia.

Euthanasia and sample collection. At selected time points, mice were deeply anesthetized by using isoflurane, and approximately 500 µL blood was collected from the retroorbital sinus into tubes containing EDTA (Becton Dickinson, Franklin Lakes, NJ). Mice then were euthanized by cervical dislocation. After euthanasia, the abdomen was opened at midline; a pipette was used to collect and measure any blood present in the peritoneal cavity. In addition, the presence of clotted blood was noted. Peritoneal lavage then was performed by using a total of 10 mL Hanks Balanced Salt Solution (Invitrogen, Grand Island, NY) containing 1:100 heparin sodium (1000 USP U/mL; Abraxis, Schaumberg, IL). The solution was pipetted into and then retrieved from the abdomen in 2-mL aliquots. Lavage fluid was retained for further analysis. The abdomen then was opened completely. All of the abdominal and thoracic organs were examined for signs of injury. The liver was examined, and injured lobes were recorded. The surface areas denoted by discoloration or hematoma or both, as well as any lacerations were measured by using a caliper and recorded. The liver was removed for further inspection, and an affected lobe was sectioned by using a scalpel. A section of liver was placed in buffered formalin.

Cell counts. One tube of EDTA-treated blood was used for CBC analysis (Hemavet Veterinary Multispecies Hematology System, Drew Scientific, Waterbury CT). The remaining blood sample was centrifuged (2000 × *g*, 5 min) and the plasma stored at −20 °C for further analysis. The peritoneal lavage fluid was centrifuged (600 × *g*, 5 min) and the supernatant stored at −20 °C for later cytokine analysis. The cell pellet was reconstituted in 200 µL RPMI 1640 (Invitrogen, Grand Island, NY) with 0.1% heat inactivated FBS (Invitrogen) and cells were counted (model Z1, Coulter, Miami, FL) after RBC lysis (Zap-Oglobin II). Slides then were loaded with 1×10^5 cells, centrifuged (700 × *g*, 5 min), and stained (Diff-Quick, Baxter, Detroit, MI) for differential analysis (300 cells) under light microscopy.

Measurement of hepatic enzymes. ALT and AST were measured by using colorimetric assays (Teco Diagnostics, Anaheim, CA) according to the manufacturer's instructions.

Cytokine ELISA. Proinflammatory (IL6, IL1β, TNFα), antiinflammatory (IL10), and chemotactic (CXCL1/keratinocyte-derived chemokine [KC] and CXCL2/macrophage inhibitory protein 2α) cytokines were examined. Cytokines in plasma (1:10 dilution) and peritoneal lavage fluids (1:2 dilution) were measured by using sandwich ELISA. Matched pairs (biotinylated and nonbiotinylated) of antimurine antibodies and their recombinant proteins (R and D Systems, Minneapolis, MN) were used according to methods previously described by this laboratory.[13] Peroxidase-conjugated streptavidin (Jackson ImmunoResearch Laboratories, West Grove, PA) and the color reagent TMB were used as the detection system. The reaction was stopped by using 1.5 N sulfuric acid, and the absorbance was read at 465 and 590 nm.

Histology. The liver samples were fixed in formalin, embedded in paraffin, and sectioned. Slides were stained with hematoxylin and eosin. The tissue sections were examined for morphologic changes under light microscopy, and photomicrographs were obtained.

MRI. Under isoflurane anesthesia, mice were placed in ventral recumbency for MRI examination by using a 7.0-T scanner (33-cm horizontal bore; Agilent, Palo Alto, CA). Body temperature was maintained by using forced heated air. A quadrature volume radiofrequency coil with an internal diameter of 35 mm was used to scan the liver of each mouse.

Axial T2-weighted images were acquired by using a fast spin-echo sequence with the following parameters: repetition time, 3000 ms; echo time, 30 ms; number of echoes, 8; field of view,

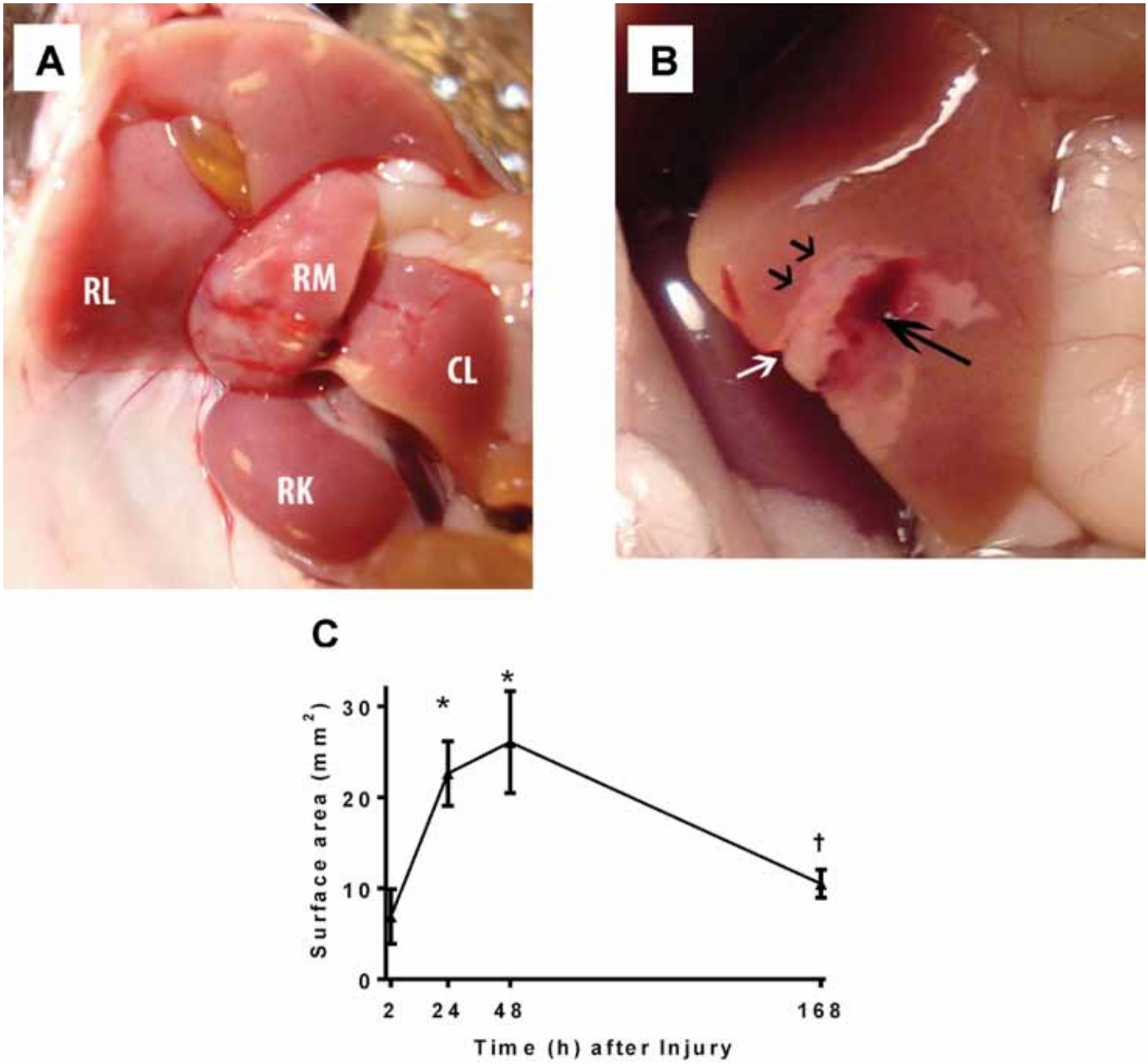

Figure 4. Characterization of hepatic surface lesions after blunt trauma. Anesthetized mice received blunt abdominal force delivered to the right side and were euthanized at various time points thereafter. (A) The subsequent lesions were confined to the right lateral (RL), right medial (RM), and caudate lobes (CL), with no apparent damage to the right kidney (RK) or other organs. (B) The lesions included hematomas (large black arrow), discolorations (small black arrows), and lacerations (white arrow). (C) The surface areas of discolored lesions were measured by using a caliper. The affected surface area appeared to increase over the first 24 to 48 h after impact and significantly (*, $P < 0.05$ as compared with the value at the 2-h time point) decreased by 7 d after trauma (†, $P < 0.05$ as compared with the value for the 48-h group). Data are expressed as mean ± SEM ($n = 5$ per group).

30 mm × 30 mm; matrix, 256 × 128; slice thickness, 1 mm; number of slices, 20 contiguous; number of scans, 1; and total scan time, approximately 3 min. Additional axial T1-weighted images were acquired by using a gradient-echo sequence with the following parameters: repetition time, 350 ms; echo time, 4 ms; flip angle, 40 degrees; field of view, 30 mm × 30 mm; matrix, 128 × 128; slice thickness, 1.0 mm; number of slices, 20 contiguous; and total scan time, approximately 1 min. Both sequences were acquired by using spatial saturation band of 7 mm thickness placed just superior to the slice package.

Statistical analysis. Student *t* test was used to compare the control group with hepatic trauma groups for analysis of CBC results. One-way ANOVA was used to evaluate multiple groups and changes over time. Differences were confirmed with a post hoc Tukey test for pairwise comparisons. Data were analyzed by using Prism version 5.00 for Windows

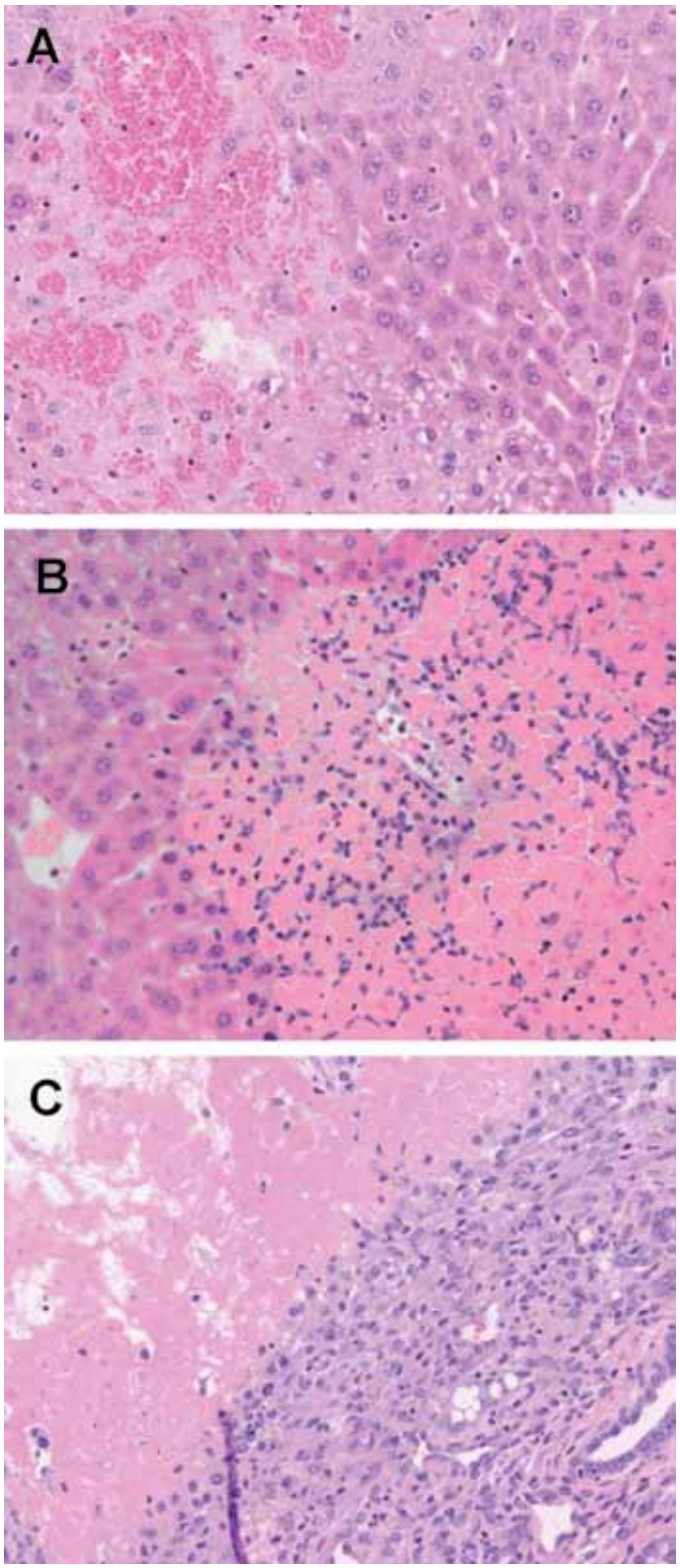

Figure 5. Histologic description of hepatic lesions. The liver was removed from mice at various time points after blunt abdominal trauma. (A) At 2 h after blunt-force trauma, the liver parenchyma has well-defined areas in which the normal architecture and cell structure appear necrotic, with little evidence of a local inflammatory reaction. (B) Within 24 h, the areas of necrosis have been infiltrated by polymorphonuclear cells. (D) After 7 d, the areas of necrosis are well-demarcated and surrounded by distinct bands of inflammatory cells, many of which are mononuclear. Photomicrographs are representative of at least 3 animals per group; magnification, 40×.

(GraphPad Software, San Diego, CA) and expressed as mean ± SEM.

Results

In the initial pilot series, the optimal settings for the cortical contusion device were determined to be a velocity of 6 m/s, with a depth of 12 mm. Under these settings, the contusion procedure was performed on a total of 25 mice (5 in the pilot and 20 in the study groups). The mean time to anesthetic recovery was 71.0 ± 6.0 min, which was not significantly different from that of the control group (52.0 ± 9.0 min). One of the 25 mice did not recover from anesthesia, and necropsy revealed severe hemorrhage associated with the hepatic trauma. The other 24 mice recovered from anesthesia and survived to their assigned time points, for an overall mortality rate of 4%. Body weight was recorded for mice in the contusion groups (n = 5 per group). Mice demonstrated significant (P = 0.0001) weight loss during the first 24 h after injury compared with that prior to injury, with a moderate (P = 0.018) rebound by day 2 and complete rebound by day 4 to control levels (Figure 2). Subjective observations of behavior and appearance (posture, coat condition) suggested no overt abnormalities by day 2.

Plasma ALT and AST. Within 2 h of hepatic injury, both ALT and AST levels were significantly (P < 0.05) elevated as compared with those from noninjured control mice (Figure 3). By 24 h, ALT returned to levels comparable to those of control mice, whereas AST levels returned to normal within 48 h.

Gross lesions. At 2 h after trauma, the amount (mean ± SEM) of easily retrievable blood in the abdomen was 111.2 ± 40.0 µL. Assuming the total blood volume to be 8.0% of body weight, the total amount of blood in retrieved from the abdomen was 6.0% ± 2.1% of total blood volume, although very small amounts of blood were not retrievable by using this method. Blood was not found free within the abdominal cavity at later time points, suggesting the reabsorption of shed blood. A complete evaluation of the abdominal contents demonstrated no apparent lesions on the body wall or of organs other than the liver. Liver injuries included hematomas, discolorations, and lacerations of the right lateral, right medial, and caudate lobes (Figure 4 A and B); the median number of lobes affected was 2. Hematomas with an average surface area of 2.3 ± 0.8 mm^2 were noted at 2 h after trauma but were no longer found at 24 h or greater. Over the first 24 to 48 h after trauma, white or yellow areas of surface discoloration significantly (P < 0.05) increased in size as compared with that at the 2-h time point and then returned to their original size by 7 d (Figure 4 C). Lacerations were either linear or stellate. The lengths of the lacerations at 2 h (3.32 ± 0.39 mm), 24 h (4.00 ± 0.55 mm), 48 h (2.80 ± 0.58 mm), and 7 d (3.17 ± 0.62 mm) after trauma did not differ between time points.

Histology. At 2 h after trauma, the surface lesions extended into the liver parenchyma. Well-defined areas of necrosis were evident, as were multifocal areas of hemorrhage (Figure 5 A). At 24 h after injury, infiltration of inflammatory cells, primarily polymorphonuclear cells, was evident within and around the necrotic areas (Figure 5 B). The findings at 48 h (not shown) were similar to those at 24 h. By 7 d after trauma, abnormal hepatic tissues

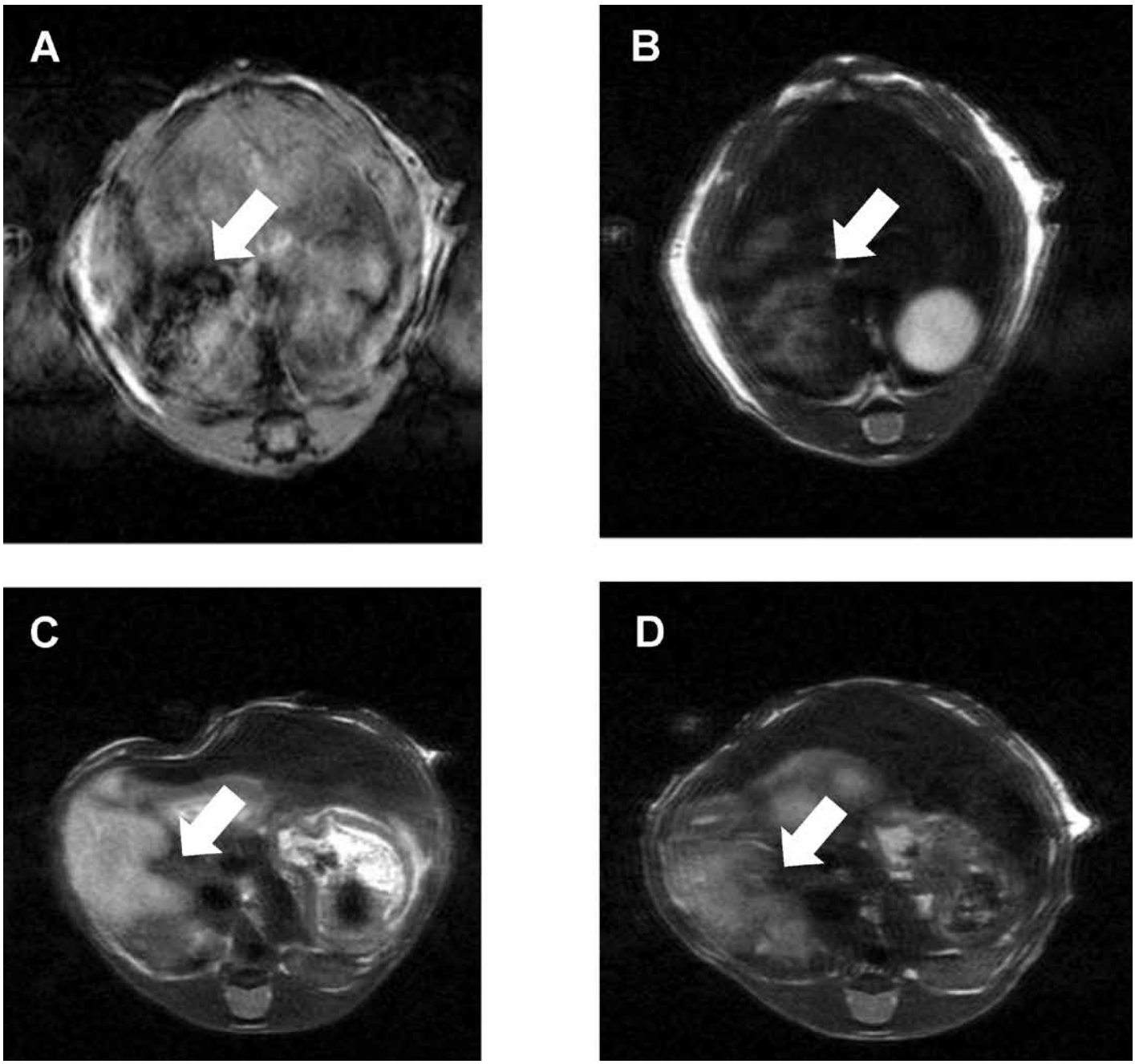

Figure 6. MRI of hepatic trauma. Images were obtained from an anesthetized mouse at various time points after hepatic trauma from a cortical contusion device. (A) T1-weighted gradient-echo image of the right lateral and medial liver lobes at 2 h after injury, showing the hypointense lesion (arrow). (B) The same lesion shown as a T2-weighted fast spin-echo axial image 2 h after trauma. (C) T2-weighted image of the hyperintense lesion (arrow) at 48 h after trauma and (D) 7 d after injury. These images are representative of those from 3 animals per time point.

were demarcated by a hypercellular zone containing both polymorphonuclear and mononuclear cell types (Figure 5 C).

MRI findings. At the 2-h time point, hepatic lesions were readily apparent in T1-weighted images as marked areas of relative hypointensity (Figure 6 A). The corresponding T2-weighted images (Figure 6 B) demonstrated the lesions as being relatively hyperintense, but these findings were not as prominent as those in the T1-weighted images. T2-weighted images demonstrated the lesions well with areas of relative hyperintensity at 48 h (Figure 6 C) and 7 d (Figure 6 D). Hyperintensity was more marked at 48 h than at 7 d. Lesions at 48 h or 7 d were not as easily identifiable in T1-weighted images as compared with T2-weighted images.

Cell counts. CBC counts were available for the control, 2-h, and 7-d groups (Figure 7). The neutrophil count for control mice did not differ significantly from those in the injured mice at the acute (2 h) and chronic (7 d) time points (Figure 7 B). Lymphocyte counts (Figure 7 C) and monocyte counts (Figure 7 D) were not significantly different from control values. Eosinophil counts in

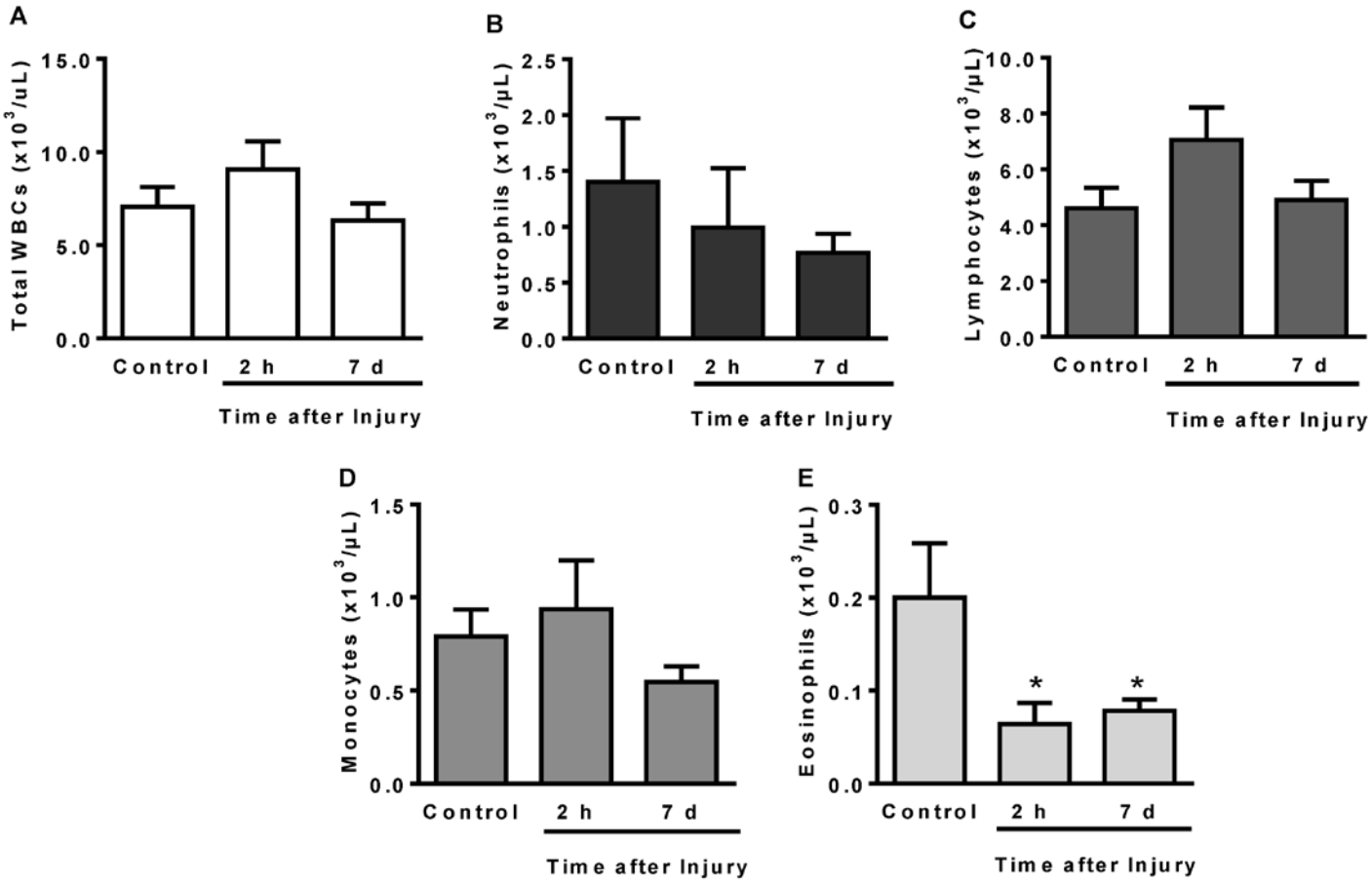

Figure 7. Peripheral WBC counts after blunt trauma. Anesthetized mice underwent blunt abdominal force and were euthanized at various time points thereafter; CBC counts were performed on retroorbital blood samples taken immediately before euthanasia. (A) Total WBC, (B) neutrophil, (C) lymphocyte, and (D) monocyte counts after trauma were not significantly different from those before surgery (control values). (E) Eosinophil counts decreased (*, $P < 0.05$ compared with the value for the control group) after injury and remained low over the course of the study. Data are expressed as mean ± SEM ($n = 5$ per group).

the peripheral blood were significantly ($P < 0.05$) lower after trauma as compared with control counts and remained significantly ($P < 0.05$) lower at 7 d (Figure 7 E).

Peritoneal lavage fluid demonstrated fluctuations in cell counts over the course of the study (Figure 8). Macrophages were the predominant cell type in lavage fluid from the control mice; numbers decreased acutely after trauma and then rose significantly ($P < 0.05$) by 48 h (Figure 8 A). At the 7-d time point, the macrophage count was less than half that of the controls ($P < 0.05$). Differences in neutrophil counts were not statistically significant (Figure 8 B). Lymphocyte counts in the lavage fluid were significantly ($P < 0.05$) lower at 24 h and 7 d after trauma as compared with counts in control mice (Figure 8 C). Eosinophils in the lavage fluid from mice with hepatic injury increased significantly ($P < 0.05$) over time for the first 48 h after trauma and then returned to control levels (Figure 8 D).

Cytokines. At 2 h after injury, plasma concentrations of the proinflammatory cytokines IL6 and IL1β and the chemokine CXCL1/KC were higher ($P < 0.05$) than those of the control group (Figure 9 A through C). IL1 β and CXCL1/KC returned to control levels within 24 h, whereas IL6 was still elevated at 24 h and returned to control levels by 48 h. The antiinflammatory cytokine IL10 was significantly ($P < 0.05$) higher in plasma at 2 h after injury and returned to control levels by 48 h (Figure 9 D). In peritoneal fluid, concentrations of IL6 and CXCL1/KC increased significantly ($P < 0.05$) within 2 h of injury and returned to control levels by 48 h (Figure 10 A and B). Concentrations of the proinflammatory cytokine IL1β and the antiinflammatory IL10 in peritoneal fluid did not change significantly after injury at any time point, as compared with control concentrations (Figure 10 C and D).

Discussion

The first goal of this study was to develop a reliable, reproducible, and nonlethal model of blunt hepatic trauma in mice. To that end, we used a cortical contusion device previously described in models of lung contusion[14,17] to deliver a standardized force to the right side of the abdomen. This procedure reliably caused lesions in the right lateral, right medial, and caudate lobes of the liver without injury to other organs. In contrast, the swine crossbow model specifically targeted an intercostal space, resulting in rib fractures and hepatic trauma in most pigs.[20] Our mouse model exhibits several similarities with trauma patients who sustain blunt hepatic injuries. The lesions were similar to those in humans and included hematomas, lacerations, and discolorations of the hepatic parenchyma with some intraabdominal bleeding. Most he-

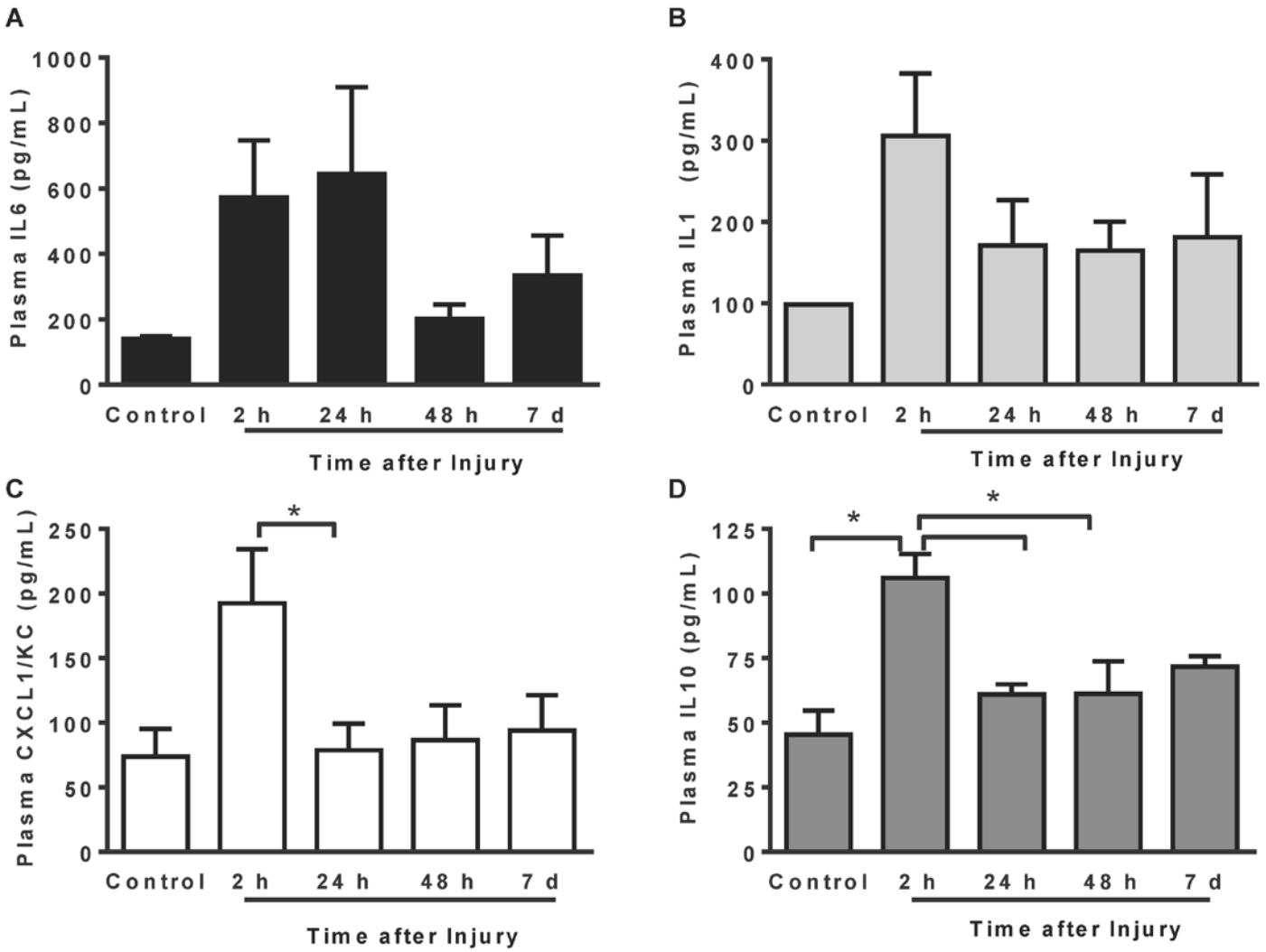

Figure 8. Peritoneal WBC counts after blunt trauma. At various time points after blunt force trauma, anesthetized mice were euthanized, and peritoneal lavage was performed for cell counts and differentials. (A) Macrophages. (B) Neutrophils. (C) Lymphocytes. (D) Eosinophil. Data are expressed as mean ± SEM (n = 5 per group); *, $P < 0.05$ between groups.

patic injuries (85%) in humans are grade I through III in nature, are hemodynamically stable, and managed nonoperatively with minimal resuscitation.[9] Bleeding generally subsides spontaneously.[9] The mouse model we describe here is categorized best as grade II to III injury[4] and was not accompanied by any need for administration of resuscitative crystalloids.

After developing our model, we were able to characterize specific immune parameters in the systemic and local compartments, with a primary focus on acute immune responses. In human trauma patients, neutrophil numbers and functions such as oxidative burst increase significantly within 24 h of injury and remain elevated for at least 96 h.[8] Trauma patients also demonstrate significant decreases in peripheral blood T cells within 24 h, persisting for at least 96 h.[8] In addition, human patients show early plasma increases in proinflammatory cytokines[7] in proportion to the severity of the injury.[12] In patients with severe blunt trauma, plasma levels of IL6 increased within 6 h and then declined in 48 h, whereas IL1β elevations were slight and remained unchanged for 48 h.[7] Similarly, in a study that evaluated trauma patients at the scenes of accidental injury, plasma IL6 levels were already elevated at 2 h after trauma and resolved over 72 h.[5] Elevated plasma concentrations of the antiinflammatory cytokine IL10 have been documented in trauma patients[18] and found as early as the time of hospital arrival.[16] Trauma-associated suppression of lymphocyte counts and increases in IL10 levels may be contributing factors to complications such as immunosuppression and sepsis.[12,15] There are currently no specific data regarding cytokine profiles from isolated hepatic trauma in human subjects. However, our model did produce inflammatory responses and cytokine profiles that are similar to those seen in human patients with multisystem trauma.[7,8,12,16,18] Plasma levels of proinflammatory cytokines (IL6, IL1β, CXCL1/KC) increased early, and the plasma IL10 levels remained elevated for the first 48 h after trauma in our injured mice. Likewise, the peritoneal proinflammatory cytokine profile of our model increased acutely after trauma. The cytokine values in the peritoneal cavity at the 2-h time point most likely were higher than those measured because free blood was retrieved for measurement prior to lavage. In our model, peripheral cell counts

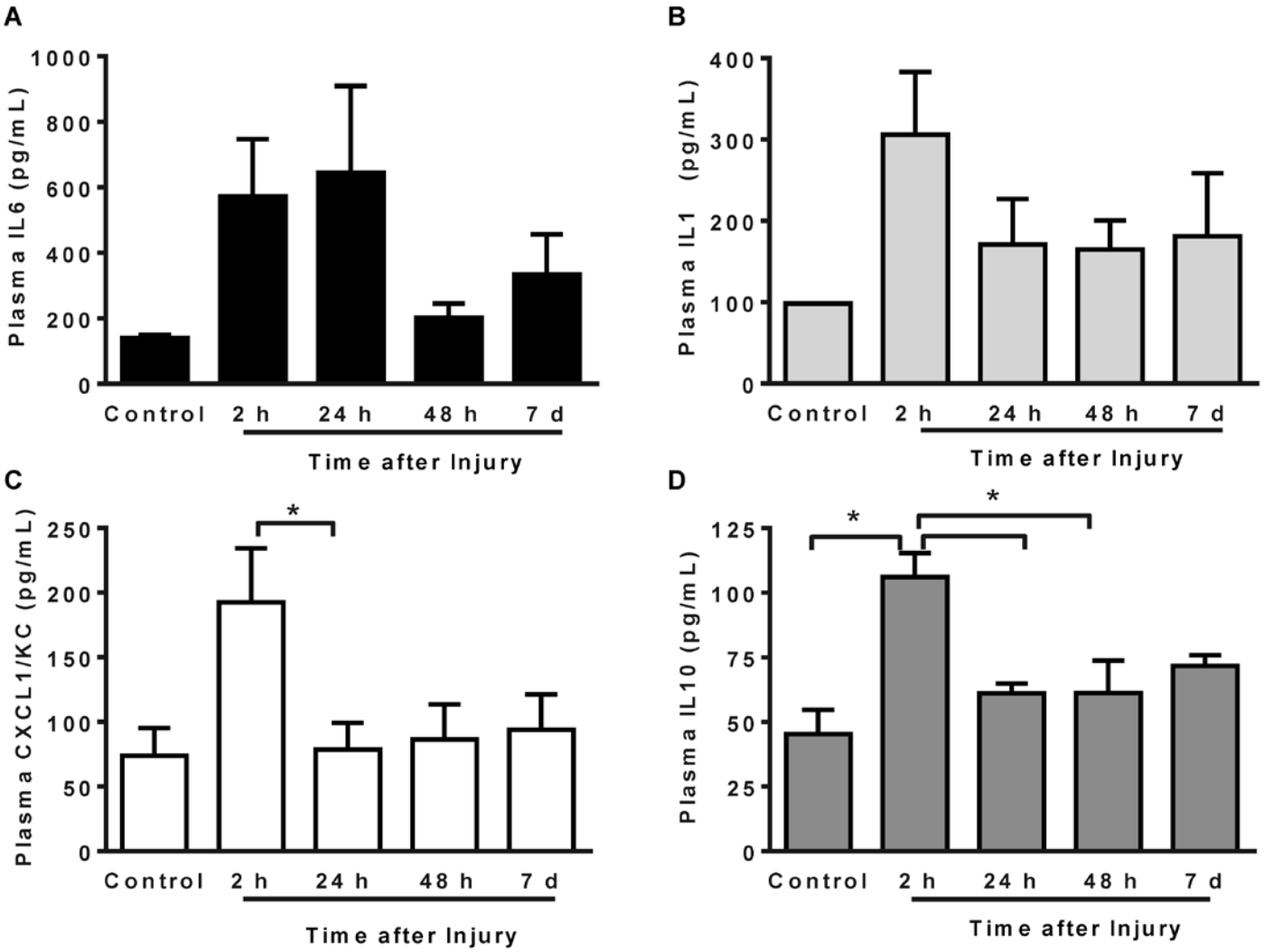

Figure 9. Plasma cytokine levels after blunt trauma. Plasma was obtained from anesthetized mice at various time points after blunt injury to the liver, and ELISA were performed for detection of the proinflammatory cytokines (A) IL6, (B) IL1β, and (C) CXC1/KC and (D) the antiinflammatory cytokine IL10. Data are expressed as mean ± SEM (n = 5 per group); *, $P < 0.05$ compared with value for control group.

did not change significantly, suggesting a mild systemic response. This finding may reflect species-associated differences or differences in the severity of injury as compared with data from humans with hepatic injury. Differential cell counts from peritoneal lavage fluid of injured mice showed increases in neutrophils and prolonged decreases in lymphocyte counts. Taken together, these data from our mouse model revealed an acute inflammatory reaction accompanied by antiinflammatory changes, as is seen in human trauma patients, and may offer a mechanism to define the specific role of the liver in the immune response to trauma. Additional work is needed to define the chronic immune sequelae of liver injury in the presented mouse model.

To refine the serial evaluation of liver injury in our model, we examined the use of MRI. In human trauma cases, the standard diagnostic tool for evaluation of liver trauma is CT, [1] which has high sensitivity and specificity and can identify hemoperitonuem as well as various hepatic lesions.[1] We evaluated MRI for sequential monitoring because of its availability and its performance in assessing soft-tissue injuries. In addition, at our institution, the MRI unit has gating capabilities that are valuable for reducing respiration artifact. At each time point, mice tolerated the isoflurane anesthesia and imaging procedure without adverse consequences. The anesthetic gas requirements were lower at the 2-h time point as compared with later time points, probably due to lingering effects of injectable anesthesia and blood loss at the early time point. Some motion artifact was apparent on the images; however, respiratory gating required prolonged anesthesia and did not dramatically improve the images. Consequently, motion artifacts associated with respiration were minimized by using spatial saturation, and doing so produced adequate images. T1-weighted images appeared most informative at 2 h after injury, because of signal void. This signal void likely resulted from hemorrhage, because deoxyhemoglobin has relatively weak magnetic properties.[19]As inflammatory cells infiltrated and the lesion organized, T2-weighted images demonstrated the extent of injury better than did T1 weighted images. The relative hyperintensity of the lesions on the T2-weighted images was consistent with necrosis and inflammation. Higher tissue water content results in

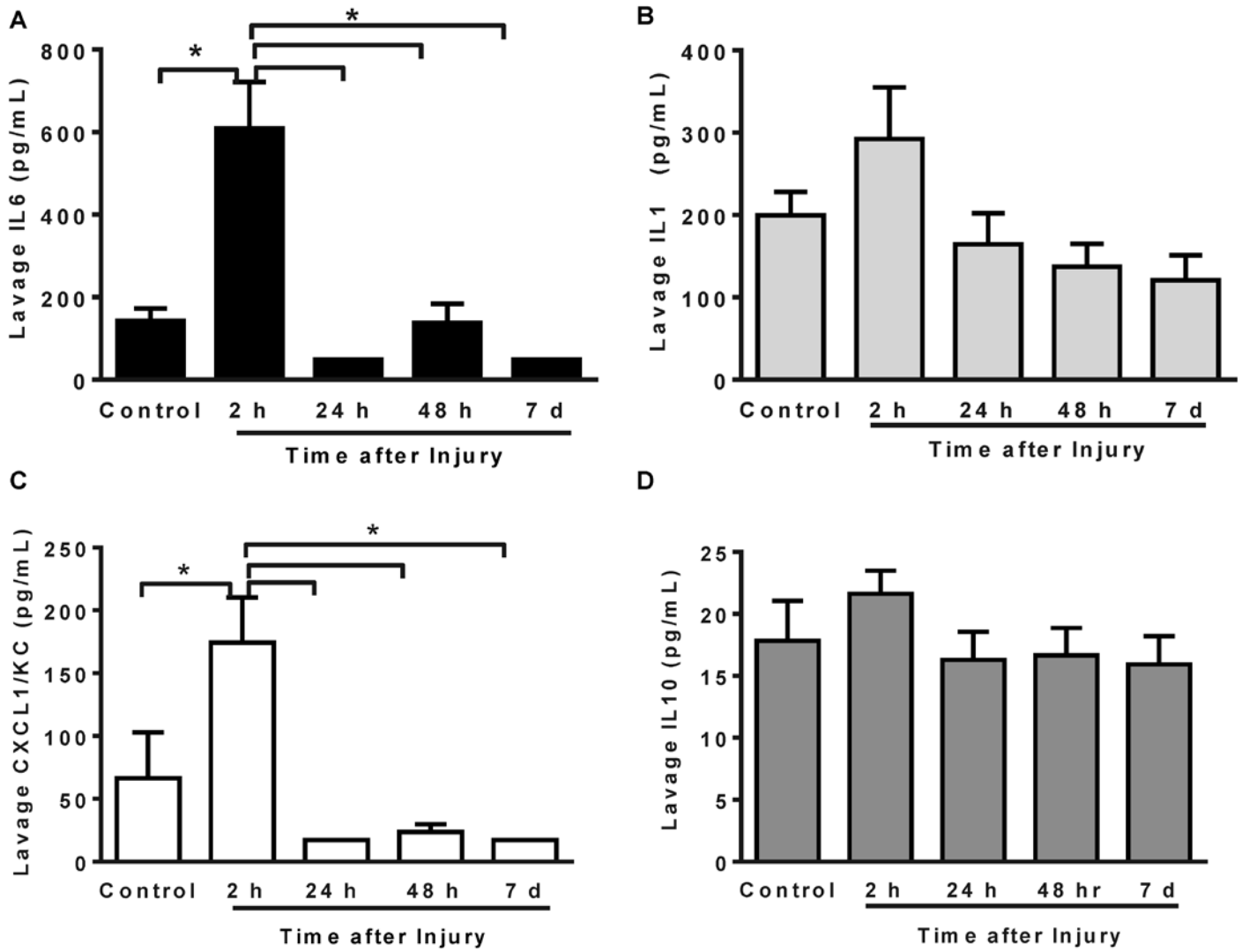

Figure 10. Peritoneal cytokine levels after blunt trauma. Peritoneal lavage fluid was obtained from anesthetized mice at various time points after blunt injury to the liver, and ELISA were performed for detection of the proinflammatory cytokines (A) IL6, (B) IL1β, and (C) CXC1/KC and (D) the antiinflammatory cytokine IL10. Data are expressed as mean ± SEM (n = 5 per group); *, $P < 0.05$ between groups.

longer relaxation times, making the lesion hyperintense relative to normal tissue in T2-weighted images.[19] Overall, MRI appears to be a useful tool for sequential monitoring of lesion volume in our mouse model of hepatic trauma.

In conclusion, we produced a reliable, low-mortality model of liver injury in mice by using a cortical contusion device. The gross lesions and overall cytokine responses were similar to those that occur in humans after blunt abdominal trauma. This model may be valuable in investigations of the molecular pathogenesis of liver injury and its sequelae, leading to new therapeutic and treatment options for trauma patients.

References

1. **Badger SA, Barclay R, Campbell P, Mole DJ, Diamond T.** 2009. Management of liver trauma. World J Surg **33:**2522–2537.
2. **Camprodon R, Solsona J, Guerrero JA, Mendoza CG, Segura J, Fabregat JM.** 1977. Intrahepatic vascular division in the pig: basis for partial hepatectomies. Arch Surg **112:**38–40.
3. **Cox JM, Kalns JE.** 2010. Development and characterization of a rat model of nonpenetrating liver trauma. Comp Med **60:**218–224.
4. **Feliciano DV, Mattox KL, Jordan GL Jr, Burch JM, Bitondo CG, Cruse PA.** 1986. Management of 1000 consecutive cases of hepatic trauma (1979–1984). Ann Surg **204:**438–445.
5. **Gebhard F, Pfetsch H, Steinbach G, Strecker W, Kinzl L, Bruckner UB.** 2000. Is interleukin 6 an early marker of injury severity following major trauma in humans? Arch Surg **135:**291–295.
6. **Heuer M, Taeger G, Kaiser GM, Nast-Kolb D, Kuehne CA, Ruchholtz S, Lefering R, Paul A, Lendemans S; Trauma Registry of the DGU.** 2009. Prognostic factors of liver injury in polytraumatic patients. Results from 895 severe abdominal trauma cases. J Gastrointestin Liver Dis **18:**197–203.
7. **Hoch RC, Rodriguez R, Manning T, Bishop M, Mead P, Shoemaker WC, Abraham E.** 1993. Effects of accidental trauma on cytokine and endotoxin production. Crit Care Med **21:**839–845.
8. **Kasten KR, Goetzman HS, Reid MR, Rasper AM, Adediran SG, Robinson CT, Cave CM, Solomkin JS, Lentsch AB, Johannigman JA, Caldwell CC.** 2010. Divergent adaptive and innate immunological responses are observed in humans following blunt trauma. BMC Immunol **11:**4.
9. **Malhotra AK, Fabian TC, Croce MA, Gavin TJ, Kudsk KA, Minard G, Pritchard FE.** 2000. Blunt hepatic injury: a paradigm shift from

operative to nonoperative management in the 1990s. Ann Surg **231:**804–813.

10. **Moore EE, Cogbill TH, Jurkovich GJ, Shackford SR, Malangoni MA, Champion HR.** 1995. Organ injury scaling: spleen and liver (1994 revision). J Trauma **38:**323–324.
11. **Murray CJ, Lopez AD.** 1997. Alternative projections of mortality and disability by cause, 1990–2020: Global Burden of Disease Study. Lancet **349:**1498–1504.
12. **Neidhardt R, Keel M, Steckholzer U, Safret A, Ungethuem U, Trentz O, Ertel W**. 1997. Relationship of interleukin-10 plasma levels to severity of injury and clinical outcome in injured patients. J Trauma **42:**863–870.
13. **Nemzek JA, Siddiqui J, Remick DG.** 2001. Development and optimization of cytokine ELISA's using commercial antibody pairs. J Immunol Methods **255:**149–157.
14. **Raghavendran K, Notter RH, Davidson BA, Helinski JD, Kunkel SL, Knight PR.** 2009. Lung contusion: inflammatory mechanisms and interaction with other injuries. Shock **32:**122–130.
15. **Sherry RM, Cue JI, Goddard JK, Parramore JB, DiPiro JT.** 1996. Interleukin 10 is associated with the development of sepsis in trauma patients. J Trauma **40:**613–616, discussion 616–617.
16. **Stensballe J, Christiansen M, Tonnesen E, Espersen K, Lippert FK, Rasmussen LS.** 2009. The early IL6 and IL10 response in trauma is correlated with injury severity and mortality. Acta Anaesthesiol Scand **53:**515–521.
17. **Suresh MV, Yu B, Machado-Aranda D, Bender MD, Ochoa-Frongia L, Helinski JD, Davidson BA, Knight PR, Hogaboam CM, Moore BB, Raghavendran K.** 2012. Role of macrophage chemoattractant protein 1 in acute inflammation after lung contusion. Am J Respir Cell Mol Biol **46:**797–806.
18. **Taniguchi T, Koido Y, Aiboshi J, Yamashita T, Suzaki S, Kurokawa A.** 1999. The ratio of interleukin 6 to interleukin 10 correlates with severity in patients with chest and abdominal trauma. Am J Emerg Med **17:**548–551.
19. **Tidwell AS.** 2007. Principles of computed tomography and magnetic resonance imaging, p 50–77. In: Thrall DE, editor. Textbook of veterinary diagnostic radiology, 5th ed. St Louis (MO): Saunders Elsevier.
20. **Wahl M, Gadzijev EM, Wahl J, Ravnik D, Pecar J, Pleskovic A.** 2005. An experimental model of reproducible liver trauma. Injury **36:**963–969.
21. **White GC.** 2012. Advanced patient assessment: inspection, palpation, and percussion, p 39. In: Basic clinical competencies for respiratory care. Clinton Park (NY): Delmar.